

Shallow and deep trap emission and luminescence quenching of TiO₂ nanoparticles on Cu doping

Biswajit Choudhury · Munmun Dey ·
Amarjyoti Choudhury

Received: 9 January 2013 / Accepted: 18 April 2013 / Published online: 1 May 2013
© The Author(s) 2013. This article is published with open access at Springerlink.com

Abstract TiO₂ nanoparticles with 2 and 4 % Cu are synthesized by sol–gel method. The crystalline phase and size of the nanoparticles are investigated with X-ray diffraction and transmission electron microscope. Cu-doped TiO₂ has an extended absorption ranging from UV to visible region. Doping of Cu disturbs the arrangement of oxygen ions around Ti⁴⁺ and generates oxygen vacancies. These oxygen vacancies capture electrons and form some ionized oxygen vacancy centers or F centers. These F centers form subband states extending from shallow to the deep level in the band gap of TiO₂. The visible emission peaks of pure and doped TiO₂ are mainly associated with self-trapped excitons (STEs) and F centers. We have observed that Auger type nonradiative recombination is responsible for the quenching of the UV and STE emission peak in the doped samples. The intense visible emission peaks in pure TiO₂ are due to shallow type centers whereas deep trap emission is predominant in doped samples. The intensity of UV and visible emission peaks are quenched with the increase in the doping level of Cu. Defects, Cu *d*-states, band structure of TiO₂ and low mobility of the carriers are responsible for the quenching of the emission peaks.

Keywords Oxygen vacancy · F centers · Trap centers · Auger recombination · Emission quenching

Introduction

After the remarkable success of Fujishima and Honda on the photocatalytic water splitting of water by TiO₂ anode, extensive research works are carried out on photocatalytic property of TiO₂ (Fujishima and Honda 1972; Yang et al. 2010; Wang et al. 2009; Choi et al. 1994). Pure TiO₂ is only UV sensitive because of its large band gap (3.0–3.2 eV), which makes it inefficient to utilize solar light for visible light photocatalysis (Yang et al. 2010; Wang et al. 2009). A significant amount of works have been carried out to modify the band gap of TiO₂ so that it absorbs light in the visible region. Some approaches are doping with cations and anions, preparing a mixture of anatase–rutile phases and making composite with other semiconductors (Wang et al. 2009; Choi et al. 1994; Jagadale et al. 2008; Spanhel et al. 1987; Baiju et al. 2009; Yang et al. 2007). Metal-doped TiO₂ is known as second generation photocatalyst as it shows tremendous activity in the degradation of organic pollutants (Chen and Mao 2007). Nagaveni et al. (2004) reported that Cu²⁺, V⁵⁺, Fe³⁺, Zr⁴⁺, etc. metal ion-doped TiO₂ shows improved performance in the photodegradation of 4-nitrophenol than that of commercial TiO₂. Dopant not only shifts the absorption edge of TiO₂ to the visible region but also act as efficient trap centers of carriers inhibiting charge carrier recombination (Yang et al. 2010; Jagadale et al. 2008). There are, however, reports where researchers have attributed that oxygen vacancies generated on doping enhances the photoactivity of TiO₂ (Ihara et al. 2003; Yu et al. 2002; Zhao et al. 2008). Ihara et al. (2003) claimed that oxygen vacancies contribute to the visible light photoactivity and N doping only enhances the stabilization of these oxygen vacancies. Yu et al. (2002) studied the photocatalytic decomposition of gas-phase acetone over F-doped TiO₂. They proposed that doping of F converts Ti⁴⁺ to Ti³⁺ for charge compensation.

B. Choudhury (✉) · M. Dey · A. Choudhury
Department of Physics, Tezpur University, Napaam 784028,
Assam, India
e-mail: biswajit@tezu.ernet.in

These Ti^{3+} ions reduce electron–hole recombination rate and enhance the photocatalytic activity. Zn doping increases the number of surface oxygen vacancies and thus enhances the photocatalytic activity of TiO_2 (Zhao et al. 2008). Photoluminescence (PL) spectroscopy is a useful technique to understand the presence of defects and the recombination ability of carriers. Wang et al. (2009) with PL spectroscopy confirms that doping of In^{3+} creates defect states below conduction band edge and reduces the PL intensity of TiO_2 . Doping of In^{3+} increases the separation of carriers and enhances the photoactivity of TiO_2 . In N-doped TiO_2 , Jagdale et al. (2008) observed that oxygen vacancy acts as electron trap and N atom acts as hole trap and thus, inhibits carrier recombination process and quenches the emission intensity. The nature of shallow and deep trap states and their effect on the PL and hence on the photocatalytic activity of TiO_2 have been studied. There are reports in nanocrystalline TiO_2 where it is stated that shallow trap states promote diffusion of carriers to the surface, while deep trap states enhance recombination of carriers (Wang et al. 2008; Weidmann et al. 1999). The oxygen vacancies behave both as shallow and deep trap states (Mattioli et al. 2008). Mattioli et al. (2008) theoretically calculated that in anatase TiO_2 the shallow and deep trap states are located at 1.5 and 2.5 eV from valence band maximum (VBM). Duhalde et al. (2005) theoretically studied that doping increases the formation of oxygen vacancy nearby Cu^{2+} ions.

In this article we have examined the role of shallow and deep trap states on the carrier recombination process in TiO_2 . The visible emission peaks of pure TiO_2 are mostly associated with shallow trap states. However, the intensity of deep trap emission increases and that of shallow trap emission decreases on doping with Cu. The electrons which are occupied in the shallow trap do not easily recombine and the defects lying deep act as recombination centers. These kinds of doped nanoparticles may serve as an efficient material in the removal of organic pollutants present in the atmosphere and in the waste water. The defects play an important part in the photocatalytic process since the defects prevent recombination of carriers making them available for photocatalysis. Our work suggests that shallow defect states are more important than deep trap states for photocatalysis since the shallow traps inhibit carrier recombination. We have used characterization techniques such as XRD, transmission electron microscope (TEM), UV and PL for the detail analysis of the crystalline structure and optical properties of the pure and doped nanoparticles.

Experimental

Cu-doped TiO_2 nanoparticles were prepared by sol–gel method. The synthesis started with the stirring of a

mixture solution of 10 mL titanium isopropoxide ($\text{Ti}\{\text{OCH}(\text{CH}_3)_2\}_4$) with 20 mL 2-propanol ($\text{C}_3\text{H}_7\text{OH}$) and 10 mL ethanol ($\text{CH}_3\text{CH}_2\text{OH}$). After stirring for 15 min, 1 mL of water was added to hydrolyze the isopropoxide chain. Copper nitrate solution with a copper concentration of 2 and 4 % were added to the host solution. The stirring was continued for nearly 6 h and after 6 h the solution turned into a gel. The gel was left unstirred for about 10 h and then centrifuged in water and ethanol for five times and then dried in a vacuum oven at 80 °C to get amorphous doped TiO_2 . This amorphous powder was annealed in air at 450 °C for 4 h to get Cu-doped TiO_2 nanoparticles.

The crystallographic phases of the prepared nanoparticles were analyzed with Rigaku Miniflex X-ray diffractometer equipped with $\text{CuK}\alpha$ radiation with X-ray wavelength of 1.54 Å. The scanning range was from 20° to 70° and the scan speed was 1°/min. High resolution TEM images of the prepared nanoparticles were obtained in JEOL-JEM 2100 TEM operating at an accelerating voltage of 200 kV. Energy dispersive X-ray (EDX) spectra of the samples were obtained in a JEOL JSM (Model 6390 LV) scanning electron microscope (SEM) with an INCAx-Sight (Oxford instruments) EDX detector. The UV–vis absorption spectra of the samples were obtained in diffuse reflectance (DRS) mode in a Shimadzu 2450 UV–vis spectrophotometer with BaSO_4 as the reference. Photoluminescence spectra were analyzed in a Perkin Elmer LS-55 spectrometer.

Results and discussion

X-ray diffraction analysis

The diffraction patterns of pure and Cu-doped TiO_2 nanoparticles are shown in Fig. 1. The diffraction pattern of pure TiO_2 matches with that of the anatase phase of TiO_2 (JCPDS-782486). However, minor brookite peaks are also present in between 27° and 36° for the doped TiO_2 nanoparticles (JCPDS-761934). Presence of this brookite phase indicates that doping of Cu inhibits complete formation of crystalline anatase phase. So et al. (2001) reported that low temperature solution phase synthesis results in the formation of brookite phase which undergoes transformation to anatase at high temperature. Both dopants and structural defects may take part in the slow growth of nuclei and therefore prevents formation of complete anatase phase.

TEM and EDX study

Transmission electron microscope images of 2 % Cu-doped TiO_2 nanoparticles are shown in Fig. 2a, b. The

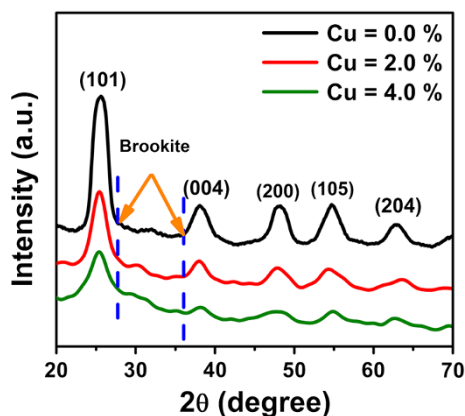


Fig. 1 X-ray diffraction pattern of pure and Cu-doped TiO₂ nanoparticles

particles are spherical in shape with aggregation. The high resolution image shows clear lattice image of the nanoparticles. The particles are not of uniform size and average number of particles is having a size of 10 nm. The EDX patterns for 2 % Cu are shown in Fig. 2c. The EDX pattern shows the presence of Cu, Ti and oxygen in the prepared nanoparticles.

UV–vis absorption study

The absorption curves of pure and Cu-doped TiO₂ nanoparticles are shown in Fig. 3. Pure TiO₂ exhibits an absorption peak at around 330 nm. Cu-doped TiO₂ also exhibits this UV absorption peak along with an absorption tail extending towards the visible region. The shifting in the absorption above 400 nm is due to the charge transfer transition from O 2*p* to the Cu *d*-states. The broad absorption hump between 450 and 900 nm is due to the *d*–*d* electronic transition of Cu²⁺ (Qiu et al. 2012). Cu²⁺ has a 3*d*⁹ electron configuration with a single electron in the *d*-orbital and the absorption hump up to 900 nm is due to the

transition of this single electron. This peak is not observed in the +1 state of Cu, since the electronic configuration became 3*d*¹⁰ and Cu would not have any electron to undergo *d*–*d* transition. This clarifies that the absorption is mainly due to Cu²⁺ state.

Photoluminescence study

The PL spectra are obtained by exciting pure and doped nanoparticles at two different excitations, 310 and 450 nm respectively. The excitation at 310 nm is the above band gap excitation and the 450 nm is below band gap excitation. Figure 4a shows the PL spectra of entire samples at an excitation of 310 nm.

The spectra contain several emission peaks. In order to understand the position and width of different emission peaks, the emission spectra of each sample are deconvoluted into five peaks by Gaussian fitting. Figure 4b–d displays the deconvoluted emission spectra of pure and doped TiO₂ nanoparticles. Each sample exhibits similar type of emission peaks and the position of entire peaks are nearly same. The UV emission peak at 390 nm is due to band to band transition of electrons from conduction band minimum to VBM, positioned at two different locations in Brillouin zone (Serpone et al. 1995). Apart from this peak, there are four visible emission peaks. The emission peaks are mostly associated with excitons and oxygen defect related shallow and deep trap centers (Lei et al. 2001; Choudhury and Choudhury 2013). The emission at 431 nm is due to self-trapped exciton (STE) (Lei et al. 2001). The STE is generated when a trapped electron on the lattice site captures a hole (Choudhury and Choudhury 2013). The STE emission may be direct or indirect. In direct STE emission, the carrier recombination is direct, while in indirect STE emission the recombination occurs via an oxygen vacancy (Iijima et al. 2008). Since Cu doping generates oxygen vacancy, the STE emission at 431 nm

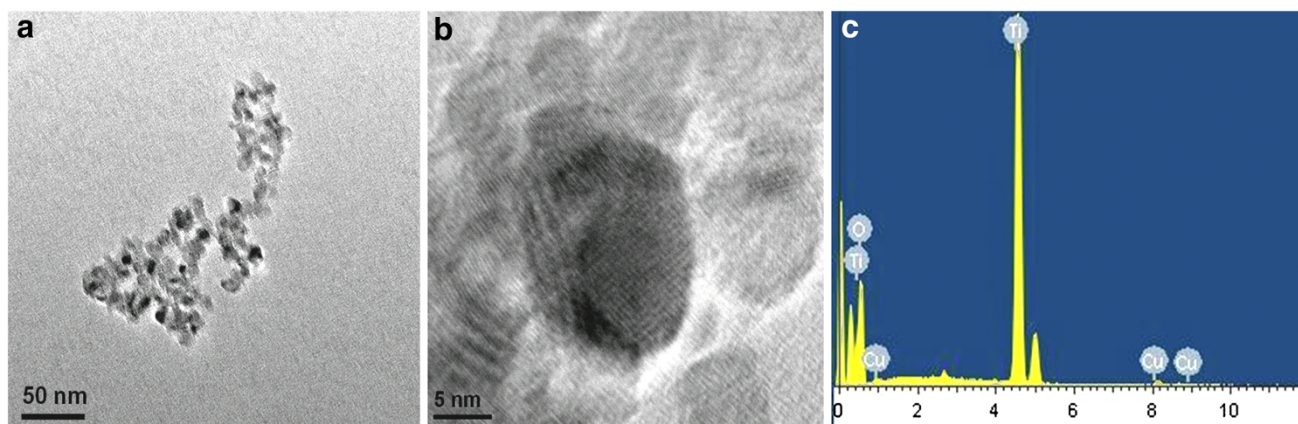


Fig. 2 Low (a) and high resolution (b) TEM images of 2 % Cu-doped TiO₂ nanoparticles. EDX pattern of c 2 % Cu-doped TiO₂ nanoparticles

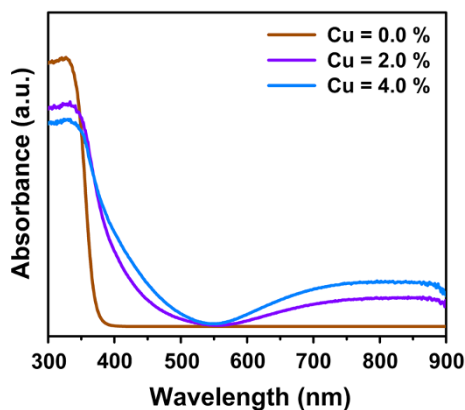


Fig. 3 UV–vis absorption study of pure and Cu-doped TiO₂ nanoparticles

may be occurring via oxygen vacancies. The emission peak at 460 and 535 nm are due to F or F²⁺ and F⁺ color centers respectively (Lei et al. 2001; Wu et al. 2010). The F center is oxygen vacancy with two trapped electrons; F⁺ is oxygen vacancy with one trapped electron and F²⁺ is the oxygen vacancy with no trapped electrons (Lei et al. 2001; Choudhury and Choudhury 2013). These oxygen defect related emissions are the result of the presence of oxygen vacancies in the shallow and deep level in the band gap of TiO₂. Sekiya et al. (2000) observed absorption at 3.0 eV (413 nm) and attributed this peak to oxygen vacancy with two trapped electrons. Kuznetsov and Serpone (2009) observed absorption peaks in the range from 2 to 2.75 eV (451–620 nm) and assigned these peaks to color centers.

We have also observed luminescence in the material on below band gap excitation. Both pure and doped TiO₂ are excited at 450 nm (2.75 eV). Figure 5 depicts the PL spectra of the samples after excitation at 450 nm. Excitation at this wavelength generates two emission peaks at 611 and at 655 nm. As mentioned the absorption peaks of

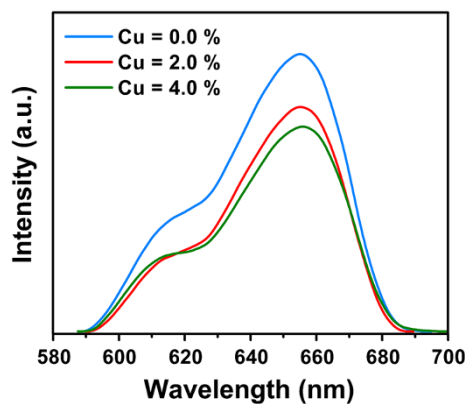


Fig. 5 PL spectra of the samples after excitation at 450 nm

oxygen defects extend from 450 to 620 nm, therefore these emission peaks are certainly associated with different types of charged (F, F⁺ or F²⁺) oxygen vacancy states. These emission peaks are the deep level emissions.

Cu doping effect on shallow and deep level emission and quenching of emission peaks

For an understanding of the doping effect of Cu on the shallow and deep trap emission, the emission intensity ratio of 536 nm (deep) to 431 nm (shallow) peak is plotted against Cu concentration (Fig. 6a). From the analysis of the PL curves, it is found that 536 nm is the deep level emission peak associated with F⁺ center and the 431 nm is the STE peak. From the plot we have found that intensity ratio of deep to shallow center increases with the increase of Cu. This infers that doping of Cu increases the radiative recombination of deep trap emission, while quenches the shallow trap emission. Both radiative and nonradiative recombination influences the efficiency of a PL emission process. The efficiency (η) of a PL process is given by

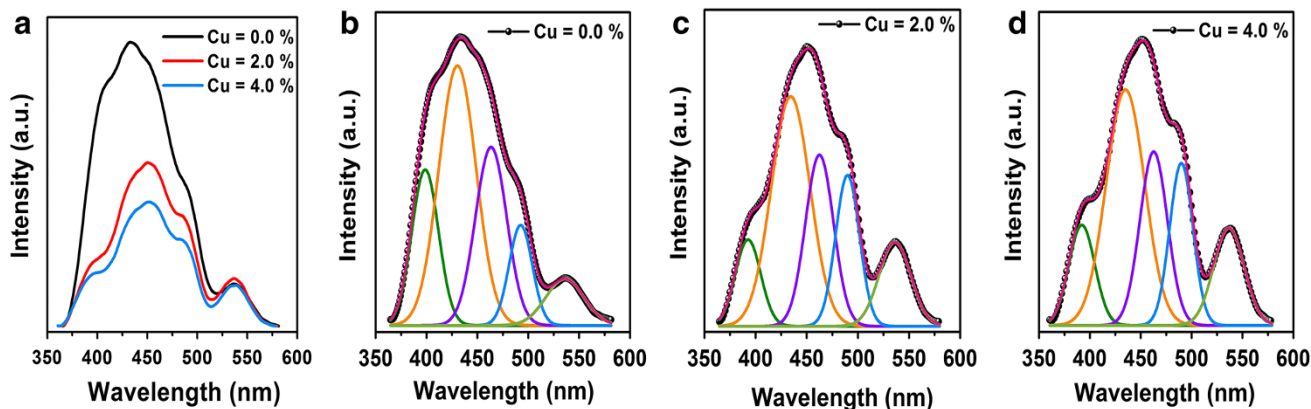
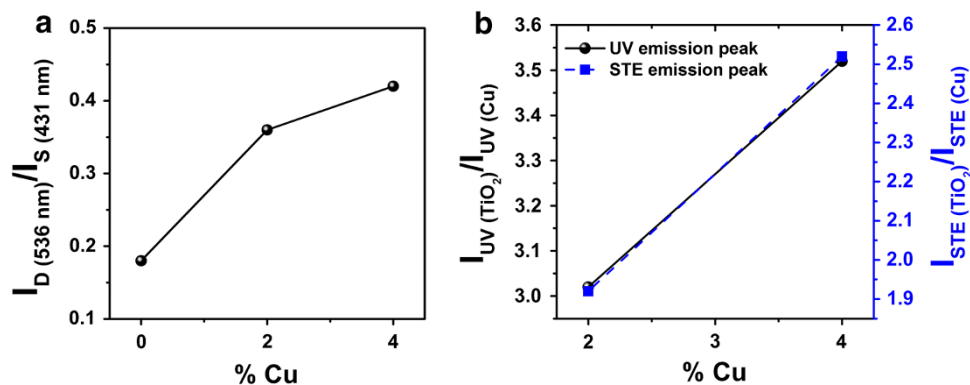


Fig. 4 Room temperature PL spectra of a pure and doped TiO₂ nanoparticles. Gaussian fitted PL spectra of b 0.0 %, c 2.0 % and d 4.0 % Cu-doped TiO₂

Fig. 6 Plot of the intensity ratio of **a** deep to shallow emission peak versus Cu loading. **b** Intensity ratio of UV and STE emission peak of pure and doped sample versus % Cu



$$\eta = \frac{I_r}{(I_r + I_{nr})} \quad (1)$$

where I_r and I_{nr} are radiative and nonradiative transition probabilities (Wang et al. 2003).

Doping of Cu increases the concentration of grain boundary defects. This observation is supported by a report of Singhal et al. (2010) who examined that oxygen vacancies generated on doping migrate to the grain boundary and thereby increases defect content in this region. Similarly, Gu et al. (2009) also reported that doping of Fe increases grain boundary defects in TiO_2 . The oxygen vacancies on the grain boundary act as nonradiative centers and form some shallow trap levels below conduction band edge. Since these defects act as nonradiative centers, the PL efficiency of the shallow trap emission decreases. Due to the charge difference between Cu^{2+} and Ti^{4+} , doping of Cu^{2+} introduces lattice site oxygen vacancies nearby Cu^{2+} ions. These Cu *d*-states and lattice site oxygen vacancies lie deep in the band gap and act as radiative recombination centers. Mattioli et al. (2008) theoretically determined that the defect levels in anatase are present both as deep (1.5 eV from VBM) and shallow (2.3 eV from VBM) levels. It is clearly seen in Fig. 4a that the quenching of the emission intensity is less towards deep emission level than that in the shallow side. There is less difference in the emission intensity of the peaks between pure and doped samples when excited at 450 nm, since at this excitation mostly deep level emissions are present. This infers that nonradiative centers are mostly present as shallow trap centers, while radiative centers are present as deep trap centers.

Although the deep trap emission intensity increases with Cu loading, the overall intensity of the emission peaks are lower than that of pure TiO_2 . This means that in comparison to pure TiO_2 the emission intensity of doped TiO_2 is quenched. Several factors may result in the reduction in the emission intensity, including the presence of trap centers, grain boundary defects, band structure and mobility of carriers, nonradiative Auger type recombination, and concentration quenching effect.

The reduction in the emission intensity of UV and STE peaks is mainly due to the Auger type nonradiative recombination process. The Auger type recombination depends on the concentration of dopants and defects in the lattice (Wang et al. 2007; Choudhury and Choudhury 2013; Dun et al. 2008). The excess free electrons, produced on doping, generate a nonradiative channel and in this channel the energy released on recombination is absorbed by a number of electrons, thereby dissipating the energy as phonons. The quenching of STE emission is due to the collapsing of the excitons. The excitons are destroyed when they undergo interaction with the lattice site defects, dopants, etc. We have plotted the intensity ratio of UV emission peak of pure and doped TiO_2 and also the intensity ratio of STE emission peak for pure and doped TiO_2 . Figure 6b shows the plot of $\frac{I_{\text{UV}(\text{TiO}_2)}}{I_{\text{UV}(\text{Cu})}}$ versus Cu and the plot of $\frac{I_{\text{STE}(\text{TiO}_2)}}{I_{\text{STE}(\text{Cu})}}$ versus Cu. We observed that the intensity ratio increases as Cu concentration increases. As it is seen, the intensity of UV as well as of STE peak decreases in the doped samples with respect to pure one. Quenching of UV emission peak indicates that the quality of the material degrades and Auger type nonradiative recombination process becomes operative on Cu incorporation.

The other defects that may affect the emission intensity are structural defects, carrier mobility, band structure, etc. (Choudhury and Choudhury 2013; Yamada and Kanemitsu 2012). From XRD it is understood that doping increases grain boundary defects. The direct confirmation is the broadening of the diffraction peak which is possible when the fraction of atoms on the grain boundary is higher as compared to those inside the grain. For bulk crystalline material we observe sharp diffraction peaks, whereas, in the nanocrystalline materials reduction in the grain size increases grain boundary content and instead of sharp peaks broad diffraction peaks may be seen. Since doping increases oxygen vacancies, these oxygen vacancies will migrate to the grain boundaries and will increase the concentration of oxygen defects in this region. Singhal et al.

(2010) in Cu-doped TiO₂ examined that the broadening of XRD peak is due to doping and defect induced fragmentation of grains that increases defects on the grain boundary. The oxygen defects on the grain boundary are randomly distributed and these defects are charged (F, F⁺ or F²⁺) and act as shallow trap centers. In addition, lattice site oxygen defects, forming deep trap centers, are also charged. The free electrons, which are not trapped in these defect centers, migrate through the lattice to recombine with the holes inside or on the surface of the nanoparticles. But the migrating electrons are strongly repelled by the charged oxygen vacancy sites and are not easily allowed to recombine with the holes. Since the concentration of these defect states increases on doping, the mobility of carriers is slowed down and the recombination process also delays. Apart from this, dopants present on the surface also stand as an obstacle for the efficient overlapping of carriers on the surface. Shah et al. (2002) and Serpone et al. (1994) observed that dopant *d*-states act as active trap centers and separate the charge carriers. The indirect band structure of anatase TiO₂ also slows down the fast recombination of the carriers. Yamada and Kanemitsu (2012) observed that the charge carriers can be efficiently separated in anatase TiO₂, since the VBM and conduction band minimum stands on different location in Brillouin zone. Doping further shifts the band edges and thus, the conduction band electrons have to traverse an indirect path for undergoing recombination with the holes. This delays the recombination and quenches the emission intensity. Apart from defects, one important phenomenon that may affect the emission intensity is concentration quenching effect. Since our emission intensity reduces with Cu, the concentration quenching effect will play an important part in the reduction of the emission intensity. In conformity to this effect, doping of ions increases the interaction among dopant and defects and form quenching centers (Katiyar and Kitai 1990). The electrons first captured by shallow trap levels jump to the Cu *d*-states. With the increase of Cu loading, the electrons jump from one *d*-state to another and then to another and thus, forms some quenching centers. The electrons, after passing through a channel of dopant and defects, ultimately find a recombination center and emit light. But, this process increases the time period for the carriers to undergo recombination and therefore reduces the emission intensity. Figure 7 shows the schematic representation of the PL emission process on excitation above (310 nm) and below band gap (450 nm).

In our analysis we observed that doping of Cu introduces shallow and deep trap centers comprising of oxygen defects and dopant *d*-states. The shallow trap centers may capture photoexcited electrons and transfer the carriers to the surface for taking part in photocatalytic process. Besides photocatalysis, presence of these shallow trap

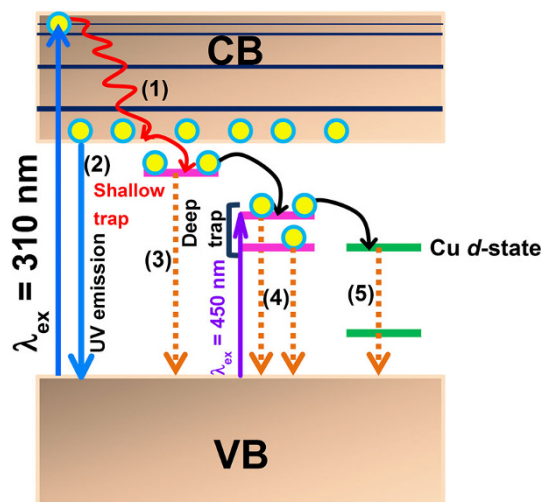


Fig. 7 Diagram showing the PL emission process on excitation at 310 and 450 nm. After excitation at 310 nm the electrons jump to the upper of the conduction band and from there jump to the bottom of conduction without emitting any light (*step 1*). From the bottom of conduction band few electrons UV light (*step 2*) and few electrons jump to the shallow trap centers and then emit light (*step 3*). The deep trap centers are either filled up by the electrons coming from shallow trap centers or got filled by the electrons excited at 450 nm. The electrons from deep trap centers may directly jump to the valence band (*step 4*) or jump to the Cu *d*-state and then recombine with the valence band holes (*step 5*)

centers make Cu-doped TiO₂ useful for photovoltaic, solar cells where carriers needs to be largely separated. Deep trap centers, on the other hand, are not suitable for these applications since emission intensity enhances due to the presence of these centers. Therefore, to be an efficient material for photocatalytic applications the Cu *d*-states and oxygen vacancies should act as shallow trap centers instead of deep traps. Our PL results also support that carrier recombination decreases, when TiO₂ is incorporated with 2 and 4 % Cu. Although photocatalytic activity of Cu-doped TiO₂ is reported before (Colong et al. 2006; Park et al. 2006), the work is not extensive and the researchers have not considered the role of the shallow and deep trap defect centers in the photocatalytic process. Therefore, we hope that the work described in this manuscript may help the readers to consider the role of defects while explaining photocatalytic activity of these nanoparticles. If the shallow trap centers are increased (by vacuum annealing or annealing in reducing atmosphere), the photocatalytic process may also be enhanced since these centers may separate the carriers.

Conclusion

From our analysis, we have come to the conclusion that doping process is beneficial for the efficient separation of

charge carriers. But, this happens only when the nonradiative trap centers near the shallow levels increases, since deep trap centers increases PL emission. The electrons trapped in the shallow trap centers can easily migrate to the surface for taking part in the photocatalytic process. The shallow trap centers are mostly oxygen defects, dopants present on surface. Cu loading not only increases shallow trap centers but also decreases mobility of the carriers and affect the band structure, thereby helps in the efficient separation of carriers. The dopant-related concentration quenching effect also inhibits the recombination and reduces PL intensity in entire doped samples.

Acknowledgments We acknowledge the financial support provided by Department of Science & Technology (Nano mission), Govt. of India through the project SR/NM/NS-98/2010 (G). We also thank sophisticated instrumentation and facility center (SAIC), NEHU, Shillong for providing us the TEM facility.

Open Access This article is distributed under the terms of the Creative Commons Attribution License which permits any use, distribution, and reproduction in any medium, provided the original author(s) and the source are credited.

References

- Baiju KV, Zachariah A, Shukla S, Biju S, Reddy MLP, Warriar K (2009) Correlating photoluminescence and photocatalytic activity of mixed-phase nanocrystalline titania. *Catal Lett* 130:130–136
- Chen X, Mao SS (2007) Titanium dioxide nanomaterials: synthesis, properties, modifications and applications. *Chem Rev* 107:2891–2959
- Choi W, Termin A, Hoffmann MR (1994) The role of metal ion dopants in quantum-sized TiO₂: correlation between photoreactivity and charge carrier recombination dynamics. *J Phys Chem* 98:13669–13679
- Choudhury B, Choudhury A (2013) Tailoring luminescence properties of TiO₂ nanoparticles by Mn doping. *J Lumin* 136:339–346
- Colong G, Maicu M, Hidalgo MC, Navio JA (2006) Cu doped TiO₂ systems with improved photocatalytic activity. *Appl Catal B* 67:41–51
- Duhalde S, Vignolo MF, Golmar F, Chliotte C, Rodriguez CE, Errico LA, Cabrera AF, Renteria M, Sanchez FH, Weismann M (2005) Appearance of room-temperature ferromagnetism in Cu-doped TiO_{2-δ} films. *Phys Rev B* 72:161313
- Dun S, Lu T, Hu Y, Hu Q, Yu L, Li Z, Huang N, Zhang S, Tang B, Dai J, Resnik L, Shlimak I (2008) Effect of As doping on the photoluminescence of nanocrystalline ⁷⁴Ge embedded in SiO₂ matrix. *J Lumin* 128:1363–1368
- Fujishima A, Honda K (1972) Electrochemical photolysis of water at a semiconductor electrode. *Nature* 238:37–38
- Gu Z, Han Y, Pan F, Wang X, Weng D, Zhou S (2009) Preparation and photocatalytic activity of Fe doped TiO₂ nanopowders. *Mater Sci Forum* 610–613:248–252
- Ihara T, Miyoshi M, Iriyama Y, Matsumoto O, Sugihara S (2003) Visible light active titanium oxide photocatalyst realized by an oxygen deficient structure and by nitrogen doping. *Appl Catal B Environ* 42:403–409
- Iijima K, Goto M, Enomoto S, Kunugita H, Ema K, Tsukamoto M, Ichikawa N, Sakama H (2008) Influence of oxygen vacancies on optical properties of anatase TiO₂ thin films. *J Lumin* 128:911–913
- Jagadale TC, Takale SP, Sonawane RS, Joshi HM, Patil SI, Kale BB, Ogale SB (2008) N-Doped TiO₂ nanoparticle based visible light photocatalyst by modified peroxide sol–gel method. *J Phys Chem C* 112:14595–14602
- Katiyar M, Kitai AH (1990) Luminescence concentration quenching due to energy migration in ZnS:Mn with fixed trap density. *J Lumin* 46:227–234
- Kuznetsov VN, Serpone N (2009) On the origin of spectral bands in the visible absorption spectra of visible light active TiO₂ specimens analysis and assignments. *J Phys Chem C* 113:15110–15123
- Lei Y, Zhang L, Meng G, Li G, Zhang X, Liang C, Chen W, Wang S (2001) Preparation and photoluminescence of highly ordered TiO₂ nanowire arrays. *Appl Phys Lett* 78:1125–1127
- Mattioli G, Filippone F, Alippi P, Bonapasta AM (2008) Ab initio study of the electronic states induced by oxygen vacancies in rutile and anatase TiO₂. *Phys Rev B* 78:241201
- Nagaveni K, Hegde MS, Madras G (2004) Structure and photocatalytic activity of Ti_{1-x}M_xO_{2±δ} (M = W, V, Ce, Zr, Fe and Cu) synthesized by solution combustion method. *J Phys Chem B* 108:20204–20212
- Park HS, Kim DH, Kim SJ, Lee KS (2006) The photocatalytic activity of 2.5 wt% Cu doped TiO₂ nanopowders synthesized by mechanical alloying. *J Alloy Compd* 415:51–55
- Qiu X, Miyauchi M, Sunada K, Minoshima M, Liu M, Lu Y, Li D, Shimodaira Y, Hosogi Y, Kuroda Y, Hashimoto K (2012) Hybrid Cu_xO/TiO₂ nanocomposites as risk reduction materials in indoor environments. *ACS Nano* 6:1609–1618
- Sekiya T, Ichimura K, Igarashi M, Kurita S (2000) Absorption spectra of anatase TiO₂ single crystals heat treated under oxygen atmosphere. *J Phys Chem Solid* 61:1237–1242
- Serpone N, Lawless D, Disdier J, Herrmann JM (1994) Spectroscopic, photoconductivity, and photocatalytic studies of TiO₂ colloids: naked and with the lattice doped with Cr³⁺, Fe³⁺ and V⁵⁺ cations. *Langmuir* 10:643–652
- Serpone N, Lawless D, Khairutdinov R (1995) Size effects on the photophysical properties of colloidal anatase TiO₂ particles: size quantization or direct transitions in this indirect semiconductor? *J Phys Chem* 99:16646–16654
- Shah SI, Li W, Huang CP, Jung O, Ni C (2002) Study of Nd³⁺, Pd²⁺, Pt⁴⁺ and Fe³⁺ dopant effect on photoreactivity of TiO₂ nanoparticles. *Proc Natl Acad Sci* 99:6482–6486
- Singhal RK, Samariya A, Kumar S, Xing YT, Jain DC, Dolia SN, Deshpande UP (2010) Study of defect induced ferromagnetism in hydrogenated anatase TiO₂:Co. *J Appl Phys* 107:113916
- So WW, Park SB, Kim KJ, Shin CH, Moon SJ (2001) The crystalline phase stability of titania particles prepared at room temperature by the sol–gel method. *J Mater Sci* 36:4299–4305
- Spanhel L, Weller H, Henglein A (1987) Photochemistry of semiconductor colloids. 22. Electron ejection from illuminated cadmium sulphide into attached titanium and zinc oxide particles. *J Am Chem Soc* 109:6632–6635
- Wang YG, Lau SP, Lee HW, Yu SF, Tay BK, Zhang XH, Hng HH (2003) Photoluminescence study of ZnO films prepared by thermal oxidation of Zn metallic films in air. *J App Phys* 94:354–358
- Wang XB, Song C, Geng KW, Zeng F, Pan F (2007) Photoluminescence and Raman scattering of Cu doped ZnO films prepared by magnetron sputtering. *Appl Surf Sci* 253:6905–6909
- Wang Q, Zhang Z, Zakeeruddin SM, Gratzel M (2008) Enhancement of the performance of dye sensitized solar cell by formation of shallow transport levels under visible light illumination. *J Phys Chem C* 112:7084–7092
- Wang E, Yang W, Cao Y (2009) Unique surface chemical species on indium doped TiO₂ and their effect on the visible light photocatalytic activity. *J Phys Chem C* 113:20912–20917

- Weidmann W, Dittrich Th, Konstantinova E, Lauermann I, Uhendorf I, Koch F (1999) Influence of oxygen and water related surface defects on the dye sensitized TiO₂. *Sol Energy Mater Sol Cells* 56:153–165
- Wu WY, Chang YM, Ting JM (2010) Room temperature synthesis of single crystalline anatase TiO₂ nanowires. *Cryst Growth Des* 10:1646–1651
- Yamada Y, Kanemitsu Y (2012) Determination of electron and hole lifetimes of rutile and anatase TiO₂ single crystals. *Appl Phys Lett* 101:133907
- Yang H, Zhang K, Shi R, Tang A (2007) Sol–gel synthesis and photocatalytic activity of CeO₂/TiO₂ nanocomposites. *J Am Ceram Soc* 90:1370–1374
- Yang M, Hume C, Lee S, Son YH, Lee JK (2010) Correlation between photocatalytic efficacy and electronic band structure in hydrothermally grown TiO₂ nanoparticles. *J Phys Chem C* 114:15292–15297
- Yu JC, Yu J, Ho W, Jiang Z, Zhang L (2002) Effects of F⁻ doping on the photocatalytic activity and microstructures of nanocrystalline TiO₂ powders. *Chem Mater* 14:3808–3816
- Zhao Y, Li C, Liu X, Gu F, Du HL, Shi L (2008) Zn doped TiO₂ nanoparticles with high photocatalytic activity synthesized by hydrogen-oxygen diffusion flame. *Appl Catal B* 79:208–215